2007 SCEC Progress Report: Finite Element Models Relating Fault Slip Rates, Geodetic Deformation, Fault Geometries and Stress Evolution in the Southern California Fault System

Bradford H. Hager (PI), Massachusetts Institute of Technology
Carl Gable (co-I), Los Alamos National Laboratory
Charles A. Williams (co-I), Rensselaer Polytechnic Institute

Introduction

The primary goals of this project were to develop a scalable, documented, extendable procedure for meshing fault systems, and to evaluate the effects of fault geometry and material inhomogeneities on predicted surface deformation fields, with specific application to southern California. One of the primary motivations for this project was the desire to minimize the amount of work necessary to provide realistic models of surface deformation. We have used two separate strategies to approach the problem. First, we have refined and optimized the strategy for creating computational meshes including detailed fault geometry. Second, we have done numerical and analytical modeling in an attempt to determine how realistic the fault geometry needs to be. If we determine that smoother representations of fault geometry predict surface deformation fields that are nearly indistinguishable from the results predicted by more detailed models, the task of producing suitable meshes will be considerably easier. Similarly, if we determine that the predicted surface deformation field is relatively insensitive to variations in the elastic material properties, this dramatically reduces the range of parameters that we need to consider in forward models of elastic deformation. The ultimate goal of this project is to lay the groundwork for inversions of interseismic deformation in southern California, considering all factors of practical importance.

To achieve our goals, a number of tasks needed to be accomplished. First, we had to develop an efficient procedure for meshing complex fault systems. We then needed an effective method for setting up boundary conditions, since these are also quite complex. We then needed to provide the mesh and simulation parameters to the PyLith 1.0 finite element code, which is the simulation code used for our modeling. We also required simplified methods of assigning complex variations in material properties, since this is one of the factors we were investigating. Finally, we needed to compute corresponding analytical solutions and compare them with the analytical results to evaluate the effects of detailed fault geometry. We were able to accomplish all of these goals, as detailed below.

LaGriT to PyLith Workflow

We are using the LaGriT mesh generation package [http://lagrit.lanl.gov] to create the meshes needed for our numerical modeling. To perform the modeling itself, we are using the PyLith finite element code [http://www.geodynamics.org], which is an outgrowth of previous SCEC-funded work and is still under active development. To perform our simulations, we first needed an efficient method of creating a mesh that included complicated fault geometries. In our previous modeling efforts, we made use of the Community Block Model (CBM) to create finite element meshes. The CBM was based on the Community Fault Model (CFM), a detailed representation of southern California fault geometry provided by the Unified Structural Representation (USR) group. The CBM represents airtight volumes constructed using the geometry from the CFM. We have used CBM-based models in the past for some of our modeling work (Figure 1); however, we have encountered problems in scalability and work flow using

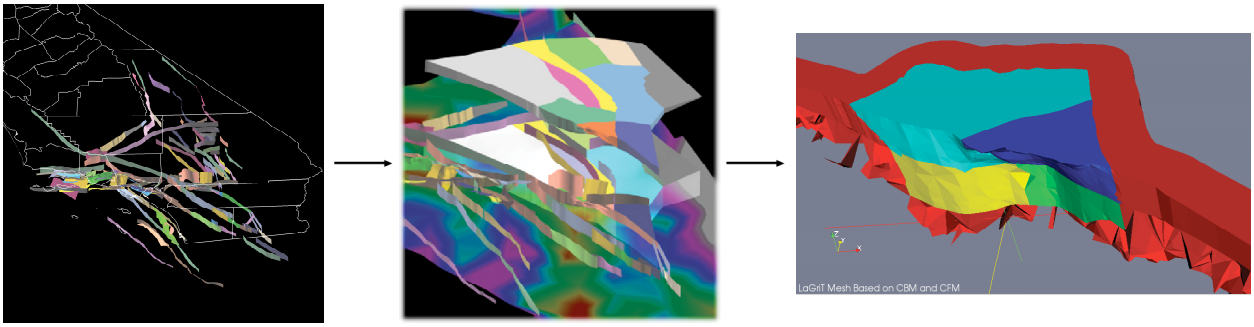

Figure 1. Simplified depiction of the steps involved in going from the CFM [http://structure.harvard.edu/cfm] (left) to the CBM [http://structure.harvard.edu/cfm] (center) to a finite element mesh of a 4-block subset of the CBM [http://meshing.lanl.gov] (right).

these types of models, particularly when dealing with a series of faults with multiple terminating splays. Furthermore, creating the CBM and updating it to correspond to the current CFM requires a significant amount of time and energy from the USR group. These issues have led us to adopt a new method of meshing where we use the CFM directly. We start by representing the entire region of interest as a closed volume and then add fault sheets that successively bisect the region. The new fault sheets are extrapolated to be close to, but not allowed to cut, existing surfaces, avoiding the pathology of mesh-mesh intersections. The approach can be iterated, adding successive levels of detail by further bisection. Using this approach, we have been able to produce meshes of southern California including as many as 90 faults.

As part of this project, we wanted to compare our finite element results to the analytical block model of *Meade and Hager* [2005] (henceforth *MH05*). To do this, the boundary conditions must be expressed in terms of rotations about Euler poles, rather than in Cartesian coordinates, as is normally done for finite element calculations. We developed two auxiliary packages for PyLith to accomplish this. The first package uses specified Euler poles in conjunction with the fault geometry provided by LaGriT to provide a spatial database that may be used directly by PyLith. The spatial database specifies the slip components in a fault-local coordinate system. An alternative package uses actual fault slips computed using the *MH05* approach, and projects them onto the more complex fault geometry used in our finite element computations.

One of the ongoing difficulties in our workflow has been providing information from LaGriT in a form that can be used by PyLith. In our most recent approach, we use GMV (Generic Mesh Viewer) output provided by LaGriT, along with pset output to define surfaces such as outer boundaries and faults. The psets are simply lists of vertices defining specified surfaces. Rather than having to provide fault orientation and additional information, as we had to do previously, this is now all handled by PyLith, which can directly use the GMV and pset information to create a properly-oriented mesh. This project has benefited from a close association with ongoing PyLith development. For example, PyLith 1.0 provided a completely new method for representing faults (cohesive elements). Since this project required a simple method of transferring fault information from LaGriT to PyLith, it was easier to develop this method as the new fault implementation was being developed.

As part of this project, we also wanted to compare surface deformations using a homogeneous elastic model against those where the elastic properties were computed using the SCEC Community Velocity Model (CVM-H, http://structure.harvard.edu/cvm-h). This database provides seismic velocity and density information for much of southern California, from which elastic properties may be computed. The brute force approach to using this database would

consist of using it externally to create a spatial database that could be used directly by PyLith. To produce the desired resolution, however, would have required a very large spatial database file, and using this file would be computationally inefficient. An alternative approach, which we have adopted, is to make use of the object-oriented nature of PyLith and extend the existing database method to include direct use of the SCEC CVM-H. This was accomplished with the help of Brad Aagaard, another of the PyLith developers. Not only has this helped with our current project, but it will also allow for the easy extension to similar databases in the near future.

Using the new meshing method, the new methods of applying boundary conditions, the new simplified LaGriT output methods, and the new database methods, we have vastly streamlined the task of setting up a PyLith simulation using complex geometries, boundary conditions, and material property variations. We have begun our investigations by applying these methods to a subset of faults in southern California including the San Andreas, Sierra Madre, and Cucamonga faults, as described in the next section.

Modeling Results

The goal of our modeling is to evaluate the effects of detailed fault geometry and material property variations on the surface deformation field predicted by elastic interseismic fault models. To do this, we have created a number of models for comparison. We first created a reference model, using the analytical model of *MH05*. This model uses the fault geometry provided by CFM-R, a rectangularized version of the CFM. This gives us a reference model that assumes a simplified fault geometry and homogeneous elastic properties. We next created a finite element model using CFM-R geometry with homogeneous elastic properties. By comparing these results to the analytical solution, we can test the accuracy of the finite element solution and also determine where the models might differ due to subtle variations in geometry or boundary conditions. We then used the same finite element model, but used the elastic property variations obtained from CVM-H. By comparing these results against the homogeneous results, we can evaluate the effects that are purely due to material property variations. To begin our investigations into the effects of detailed fault geometry, we then created a finite element model using the full geometry provided by the CFM. As for the CFM-R-based models, we ran one version of the model assuming homogeneous properties, and another version using the material property variations provided by the CVM-H. By comparing the results of all these models, we have started to gain an understanding on the importance of including material property variations and detailed fault geometry in interseismic models of surface deformation.

As mentioned above, we have used a subset of southern California faults to begin our investigation. The faults in our study include a portion of the southern San Andreas fault, the Sierra Madre fault, and the Cucamonga fault. The region of interest is shown in Figure 2, which also shows two components of the slip distribution used in our models. The slip distributions show the spatial database results used by PyLith to perform the computations. They are obtained by using the Euler pole results used for the analytical model. Since the CFM-R-based models assume a constant fault dip for each segment, the computed fault slip can be significantly different in regions where the CFM indicates significant variations in fault dip. The most obvious example is in the region of the San Gorgonio Pass, where variations in fault dip for the CFM yield significantly different dip-slip components when compared to the CFM-R-based models. Comparing the geometry for the two models, it also appears that the simplified geometry of the CFM-R-based models does not always provide a good representation of the CFM. One of the current outstanding issues is determining whether these discrepancies are due to the CFM-R

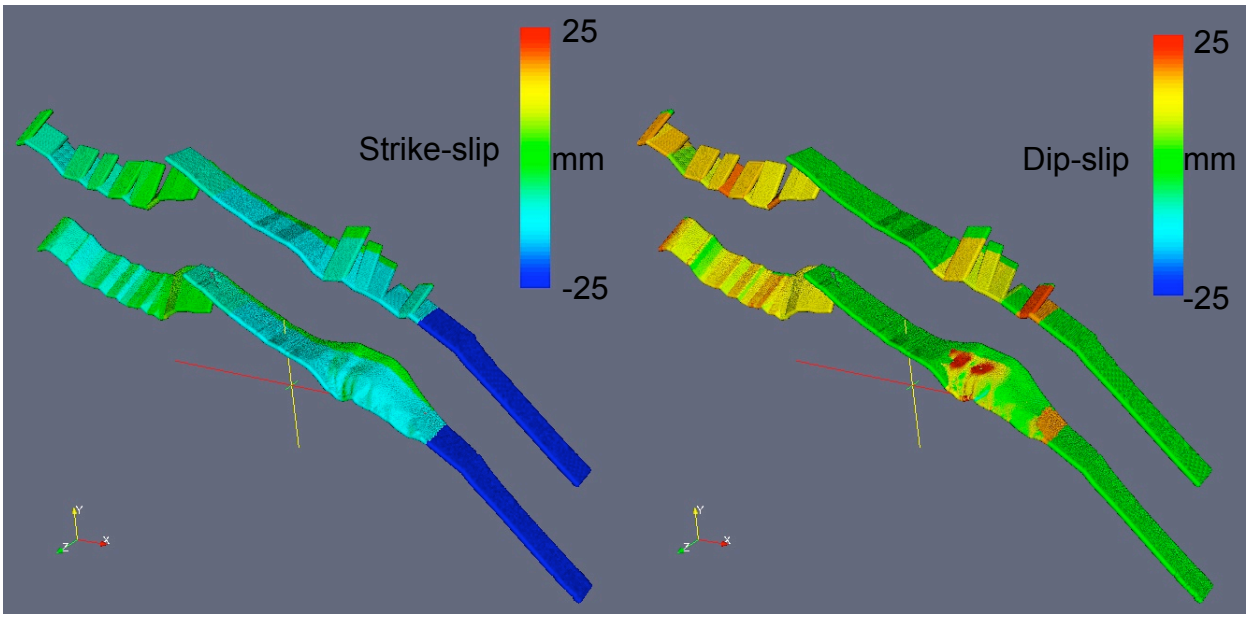

Figure 2. Strike-slip and dip-slip components used in our FEM fault models. CFM-R-based models are shown at the top, while the lower models use the full CFM. Variations in fault slip due to fault geometry are very obvious when comparing the dip-slip components in the San Gorgonio Pass region.

itself or in our interpretation of the CFM-R geometry. The most obvious discrepancies are on the Cucamonga fault and in the San Gorgonio region, where it is likely that the different fault geometries would predict significantly different surface deformation fields.

Our initial comparisons between the analytical results and those from the CFM-R-based homogeneous finite element model are qualitative, at present (Figure 3). The difficulty is that the analytical results are computed on a regular grid, while the FEM results are computed on a mesh where the resolution varies with distance from the fault. Although we can see general overall agreement between the results, we are not able to quantify the model differences at present. Our comparisons will be greatly aided by the CIGMA package being developed at CIG. This package, in addition to allowing quantitative comparisons between meshes of different resolutions, will also allow the misfit to be integrated over the mesh, which will provide a much more robust comparison method. At present, it appears that at least some of the present misfit between the models is due to a discrepancy in the geometry of the finite element mesh with respect to the fault geometry used for the analytical solution. We plan to resolve this issue in the near future.

The CFM-R-based and the CFM-based FEM results are computed on different meshes, so we are also unable to quantitatively compare these results. We will be able to quantify the differences between both the analytical and FEM models once the CIGMA package is available. A qualitative comparison of the north component of surface displacement (Figure 4) shows a few significant differences, including a slight difference along the southern San Andreas, and more significant differences on the south side of the San Gorgonio Pass and along the Sierra Madre and Cucamonga faults. The difference along the southern San Andreas is likely to be due to a small difference in the average fault dip along this region, while the difference in the San Gorgonio Pass is probably because the assumption of a constant fault dip is not a reasonable approximation for this region. It appears that the differences along the Sierra Madre and Cucamonga faults are due to discrepancies in the geometries used for the two models.

The next step was to compare the homogeneous FEM results against those where the material properties were obtained from CVM-H. In Figure 5a we show the shear modulus values obtained from CVM-H projected onto the fault surfaces. The most noticeable variations are along the southern San Andreas, where the shear modulus is relatively low along the fault, and similar smaller regions near the surface for the Cucamonga and Sierra Madre faults. These are the regions where we might expect to see significant differences between the predicted surface deformation fields. As seen in Figure 5b, where we show the model differences for the north component of the displacement field, these are precisely the regions where the greatest differences are seen. Referring to Figure 4, we see that the differences are on the order of 10% of the total displacement field, which are significant given the accuracy of the SCEC GPS velocity field. Also superimposed on the plots of Figure 5b are dots showing the locations of existing GPS sites. One of the factors to consider is whether the models predict significant differences in regions where we have observations. As seen from this figure, a significant number of existing observations lie in the regions where the models have significant differences, so the effects

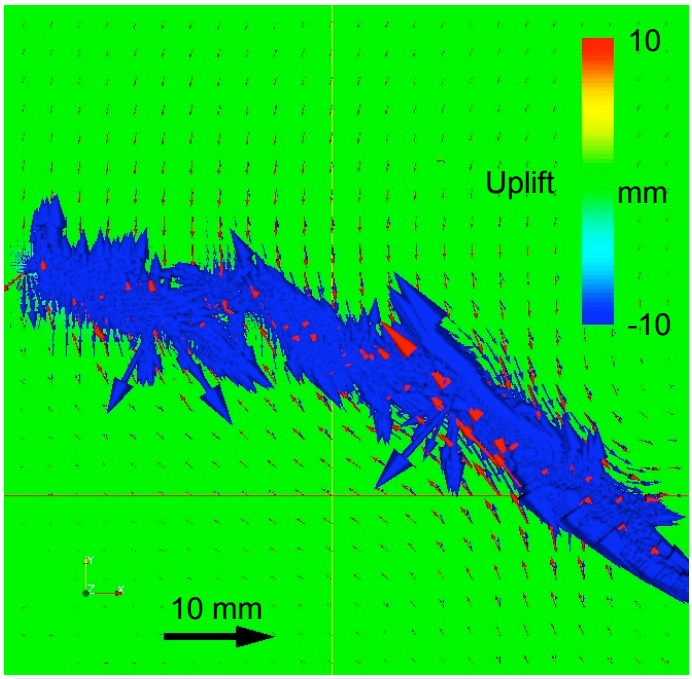

Figure 3. Comparison of analytical results (red arrows) against FEM results assuming CFM-R geometry and homogeneous material properties (Blue arrows).

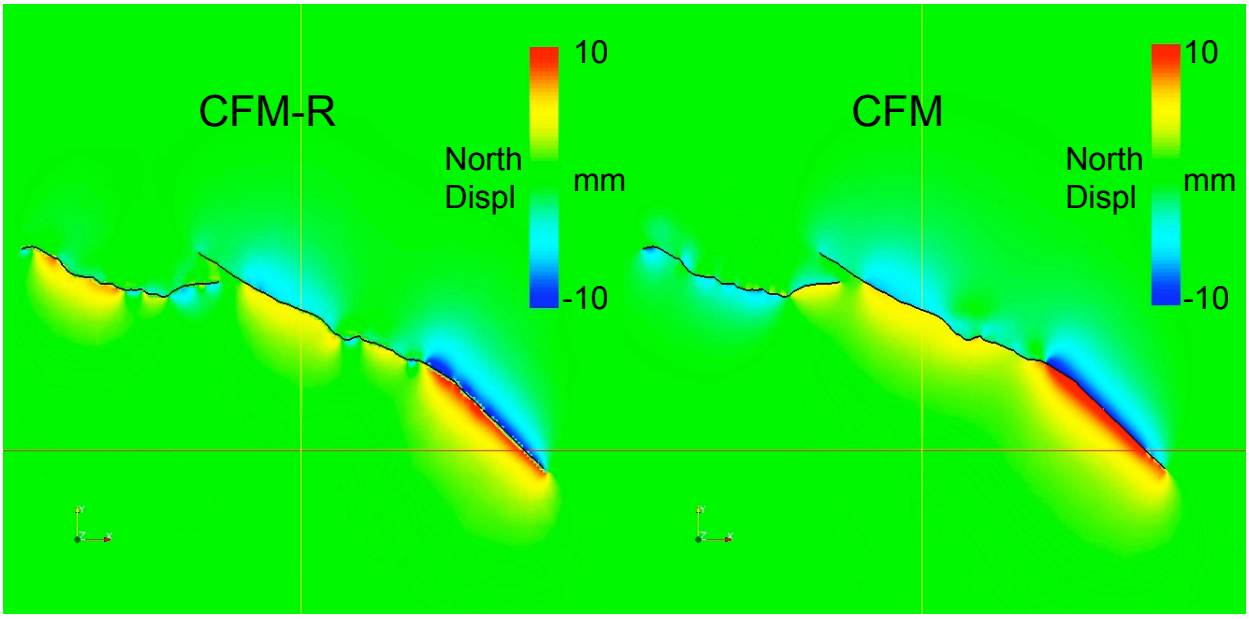

Figure 4. Comparison of predicted north displacement for CFM-R-based (left) and CFM-based (right) finite element models. The largest differences occur near the San Gorgonio Pass and along the Sierra Madre fault.

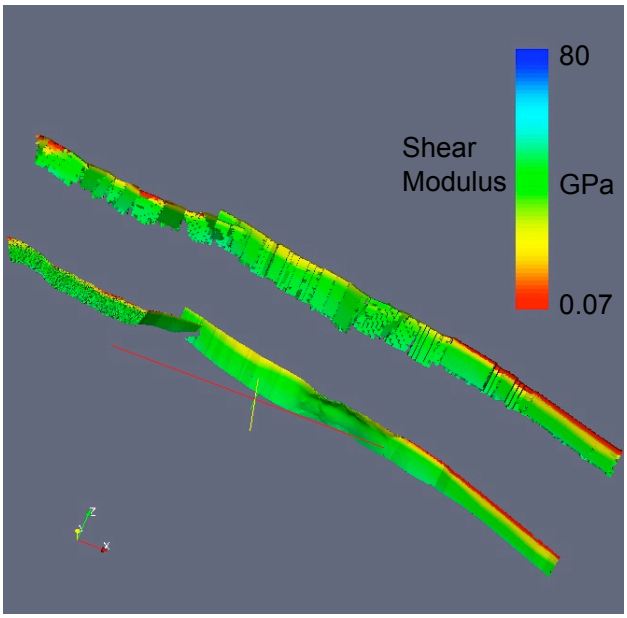

Figure 5. Figure 5a (left) shows the predicted shear modulus obtained from CVM-H projected onto both the CFM-R and CFM finite element models. Regions of low shear modulus occur along the upper portion of the southern San Andreas, as well as along the upper portions of the Cucamonga and Sierra Madre faults. This creates differences in the predicted surface deformation field in these regions, as seen in Figure 5b (bottom), where we have subtracted the CVM-H results from the homogeneous results. Observable differences occur in regions where we have GPS observations (shown with magenta dots), so we might expect to be able to detect these signals, which are on the order of 10% of the displacement field for this component.

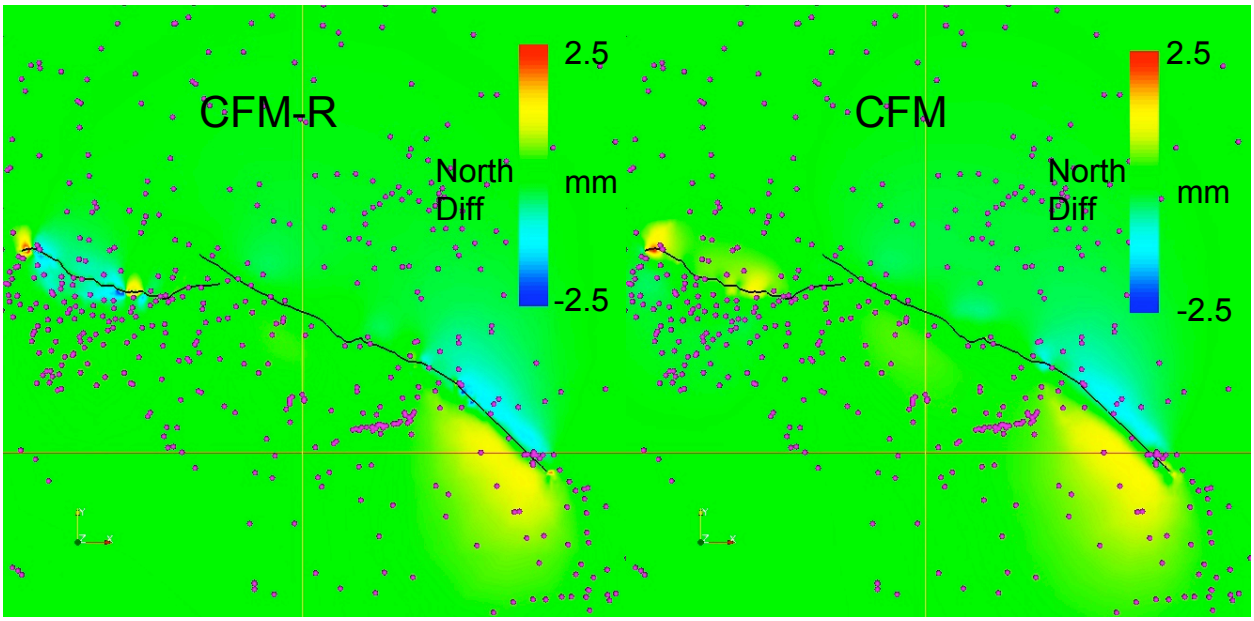

should affect inferences of fault slip rates, stressing rates, and seismic hazard.

Presentation and Dissemination of Results

We have presented the results of our meshing work, code development, and modeling work to date at the 2007 SCEC Annual Meeting [*Aagaard et al.*, 2007a; *Lu et al.*, 2007; *Parker et al.*, 2007a; *Williams et al.*, 2007a] and at the AGU Fall Meeting [*Aagaard et al.*, 2007b; *Gable et al.*, 2007; *Parker et al.*, 2007b; *Williams et al.*, 2007b], as well as at GSA [*Turner and Gable*, 2007; *Gable*, 2007]. In addition, the software created specifically for this project is now publicly available in both LaGriT [http://lagrit.lanl.gov] and as part of the PyLith package [http://www.geodynamics.org]. Some of the software additions for this project were presented at the CFEM workshop in Golden, CO, in June of 2007. More recent additions will be discussed and demonstrated at the next CFEM workshop (Golden, CO, in June of 2008). We are continuing our investigations into the effects of both fault geometry and material property variations, and this should result in two publications completely supported by this SCEC project.

This project has laid the groundwork for a number of future SCEC projects, including our own plans for much larger-scale models of southern California block dynamics as well as those of other investigators.

References

Aagaard, B., C. Williams, and M. Knepley, PyLith 1.0: A finite-element code for modeling quasi-static and dynamic crustal deformation, *SCEC Annual Meeting*, 2007a.

Aagaard, B., C. Williams, and M. Knepley, PyLith: A finite-element code for modeling quasi-static and dynamic crustal deformation, *AGU Fall Meeting*, 2007b.

Gable, C. W., B. H. Hager, J. Lu, and C. A. Williams, Finite element meshing of the SCEC Community Fault Model: Methods and algorithms, AGU Fall Meeting, 2007.

Gable, C. W., Interfacing mesh generation with 3D geologic framework models, *GSA Annual Meeting*, 2007.

Lu, J., C. W. Gable, B. H. Hager, and C. A. Williams, Implementation of finite element models using the SCEC Community Fault Model: Meshing and test computations, *SCEC Annual Meeting*, 2007.

Meade, B. J., and B. H. Hager, Block models of crustal motion in southern California constrained by GPS measurements, B. J. *J. Geophys. Res*., *110*, B03403, doi: 10.1029/2004JB003209, 2005.

Parker, J., C. W. Gable, G. Lyzenga, and C. Norton, PYRAMID automatic refinement based on GeoFEST elastic strain energy using LaGriT-meshed CFM faults, *SCEC Earthquake Simulators Workshop*, 2007a.

Parker, J., G. Lyzenga, C. Norton, P. Lundgren, and C. W. Gable, The QuakeSim GeoFEST modeling system – new features inspired by San Andreas Fault motion, *AGU Fall Meeting*, 2007b.

Turner, A. K., and C. W. Gable, A review of geological modeling (GSA Short Course), *GSA Annual Meeting*, 2007.

Williams, C., C. Gable, B. Hager, and J. Lu, Using finite element meshes derived from the SCEC Community Fault Model to evaluate the effects of detailed fault geometry and material inhomogeneities, *SCEC Annual Meeting*, 2007a.

Williams, C. A., C. W. Gable, B. H. Hager, and J. Lu, Using finite element meshes derived from the SCEC Community Fault Model to evaluate the effects of detailed fault geometry and material inhomogeneities, *AGU Fall Meeting*, 2007b.